INVESTIGATIONS ON THE GLOBAL STABILITY OF HIGH STRENGTH CONCRETE SANDWICHED SQUARE DOUBLE STEEL TUBULAR COLUMNS

MASHUDHA SULTHANA U[1] and ARUL JAYACHANDRAN S[2]

[1]*Post Doctoral Scholar, Department of Civil Engineering, Indian Institute of Technology Madras, Chennai - 600036, India.*
E-mail: mashudha@gmail.com
[2]*Professor, Department of Civil Engineering, Indian Institute of Technology Madras, Chennai - 600036, India.*
E-mail: aruls@iitm.ac.in

Lately, concrete sandwiched double steel tubular columns (CSDST) has gained focus in research. Higher strength, stiffness, ductility and fire resistance tendencies are some of the many structural-performance related advantages of this cross-section. Square CSDST is more efficient over other CSDST configurations as it simplifies connection design and offers better stability against global buckling. However, studies on the column stability of square CSDST is not found in the available literature. Therefore, the present research attempts to investigate the stability aspects of square CSDST through experimental and numerical works. Axial compressive tests are carried out on square-CSDST column specimens of length to width ratio (L/D) around 24, to capture the overall stability effects in the column. Hollowness ratios of 20%, 50% and 70% are selected as test parameters, and concrete strength of about 80 N/mm^2 is used for filling the steel tubes. Maximum axial capacity of around 1990 kN is reached for an outer specimen dimension of 150×150 mm with 3600 mm height. It proves the potential of square-CSDST in resisting global buckling. The test axial capacities are compared with code capacity equations (AISC-360 (16) ; EN 1994-1-1 2004) and it shows an over-strength of about 15% in the test results. Nevertheless, the numerical model which is developed using the measured global imperfections of the specimen is in good agreement with the experimental results.

Keywords: Overall stability, slender column, sandwiched concrete, hollowness ratio, initial imperfection.

1 Introduction

Use of tubular steel in construction industry has increased over the years due to its inherent torsional rigidity, lesser susceptibility to corrosion and structural elegance. However, local and global buckling of tubular members hinders the achievement of full design capacity. Fabrication of localized steel stiffeners in tubular cross-sections is tedious, unlike an open steel cross-section. Conventionally, concrete filling is adopted to improve the local and global stability of tubular steel (Eggemann 2003). Experimental studies have observed increase in the flexural and axial resistance of the cross-section upon concrete filling (Gardner and Jacobson 1967; Knowles and Park 1969; Sakino et al. 2004). Other important structural aspects that had improved in a concrete filled steel tubular column (CFST) are the stiffness, ductility and fire resistance properties. Concrete sandwiched double steel tube (CSDST) is a variant of CFST that has been

Proceedings of the 17th International Symposium on Tubular Structures.
Editors: X.D. Qian and Y.S. Choo

Published by Research Publishing, Singapore.
ISBN: 978-981-11-0745-0; doi:10.3850/978-981-11-0745-0_122-cd

in the research foray for the past two decades. The potential of this cross-section as a building component is found in several experimental studies (Elchalakani et al. 2002; Han et al. 2004; Lu et al. 2011; Tao et al. 2004; Uenaka et al. 2010). The higher stiffness, ductility and fire resistance properties of CSDST is evident from the experimental results. Most of the reported test data is for short column behavior studies, which found the hollowness ratio as a peculiar parameter in CSDST cross-section (Huang et al. 2010). The presence of inner steel tube and hollow space formation improves the fire resistance mechanism, and have reported to be better than a conventional CFST for slender columns (Romero et al. 2015a). On the other hand, studies on slender CSDST columns are very few (Essopjee and Dundu 2015; Romero et al. 2015b) and none for square CSDST. Therefore, the present research aims at investigating the stability aspects of slender square CSDST filled with high strength concrete through experimental and numerical works.

Experimental results of three slender square CSDST specimens are reported in this paper. The dimensions of the outer steel tube are selected such that the specimen fails in overall buckling and interaction with local buckling is avoided. The annular space between the inner and outer steel tubes is filled with high strength concrete of cube compressive strength around 80 N/mm^2. Hollowness ratio (0.2, 0.5 and 0.7) is selected as a primary parameter since it distinguishes CSDST from a general concrete filled steel tubular column (CFST). The experimental results projects the global instability of square CSDST to be inversely proportional to the hollowness ratio of the cross-section. The test axial capacities are compared with numerical model developed and code provisions in AISC-360 (16) and EN 1994-1-1 2004 with modifications for CSDST.

2 Experimental Program

The three types of square CSDST cross-sections selected for axial compression test is shown in Fig. 1. The cross-section dimensions of the inner and outer steel tubes and material property details are given in Table 1. The primary objective of this program is to study the global buckling in CFDST long columns. Therefore, tubes sizes are selected such that the specimens fail by global buckling under axial compression. A nominal diameter of 165.1 mm is selected as the outer steel tube, with three different inner steel tubes sizes to develop hollowness ratios of, 70%, 50% and 20% (Fig. 1). Length of all the specimens is 3600 mm. Material property of the steel tubes is found by fabricating and testing the coupons as per ASTM-E8/E8M 2009. The average yield and ultimate strength of the tension coupon is 400 N/mm^2 and 450 N/mm^2, respectively. Concrete compressive strength was found by casting concrete cubes (per IS:516-1959), from each concrete batch prepared for filling the specimens. Mean concrete cube strength (f_{cm}), is reported here in N/mm^2. D_o and D_i are the measured diameters (in mm) of outer and inner steel tubes respectively, and t_o and t_i are the measured thicknesses (in mm) of outer and inner steel tubes, respectively.

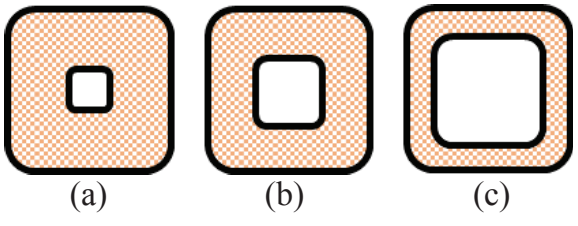

Figure 1. Selected cross-sections. (a) SS-20-80 (b) SS-50-80 (c) SS-70-80

Table 1. Geometric and material properties of the test specimens

Sp. ID	Measured size				D_o/ t_o	D_i/ t_i	f_{cm}
	D_o	t_o	D_i	t_i			
	(mm)	(mm)	(mm)	(mm)			(N/mm^2)
SS-20-80	151.05	6.1	32	2	24.76	16.00	89.02
SS-50-80	150.35	6.14	72.52	3.96	24.49	18.31	84.95
SS-70-80	149.98	6.08	100.3	3.94	24.67	25.46	87.25

2.1 *Specimen preparation and test protocol*

The steel tubes used for preparing specimens are manufactured by cold forming and cold rolling process. The 3600 mm long specimens are sensitive to imperfection along the length of the specimen. Therefore, the along-length imperfection is alone measured using a laser beam arrangement. The maximum out-of-straightness imperfection at the mid-height of the specimen is around 0.9 mm (L/4000), which is very small compared to L/1000 consideration as per code provisions (ANSI/AISC 2016; EN 1994-1-1 2004). The outer and inner steel tubes are placed coaxially by making suitable fixtures, and the ends are welded to steel plates to facilitate uniform transfer of load across the cross-section. The specimens are filled with self compacting concrete in upright position. The schematic test set-up and instrumentation of the specimens is shown in Fig. 2. Roller bars are fabricated to provide hinge type boundary condition and the surface is applied with grease to avoid frictional losses while loading (inside photograph in Fig.2).

The specimens are subjected to axial compression in a 6000 kN load-controlled compression test frame, and a 5000 kN hydraulic jack is used for loading. Axial load is applied at a rate of 130 kN/min. The displacements and strains in the test specimens are continuously recorded in a data logger.

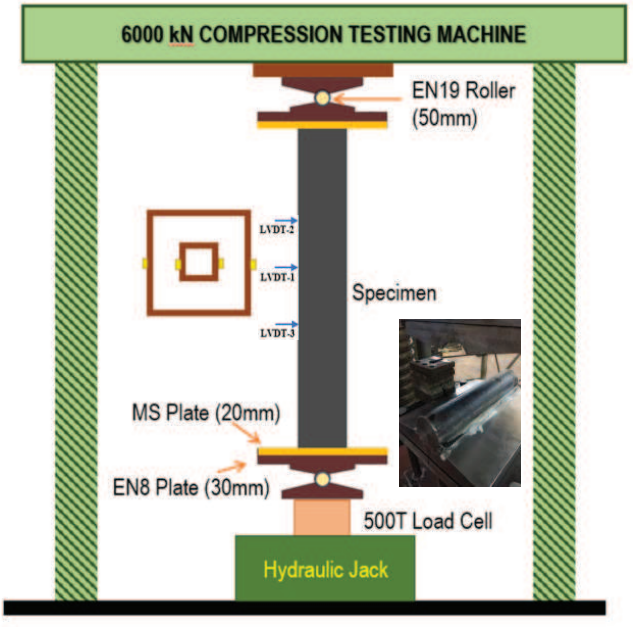

Figure 2. Schematic diagram of test set-up

2.2 *Test results*

All the three test specimens failed by global buckling. Load versus lateral deflection measured at the mid-height of the specimens is shown in Fig. 3. The failure load of the specimens from the test is given in Table 2. The test capacities are compared with CFST code provisions in ANSI/AISC 2016; EN 1994-1-1 2004 modified for CSDST to include the contribution of inner tube. The code predictions are conservative that indicate an over-strength of around 15% in the test capacities. The test results are also compared with numerical results and presented in Table 2.

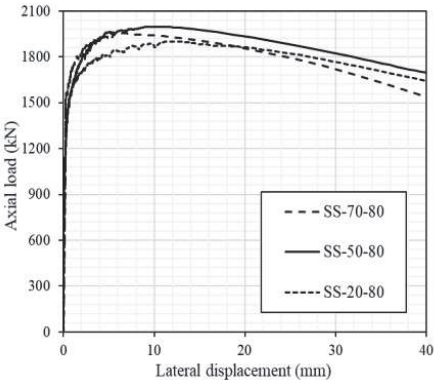

Figure 2. Test results. (a) Axial load versus axial displacement (b) Axial load versus lateral displacement

Table 2. Test axial capacity compared with code provisions and FE results

Sp. ID	P_{test}	P_{EC4}	P_{AISC}	P_{FE}	P_{EC4}/P_{test}	P_{AISC}/P_{test}	P_{FE}/P_{test}
	(kN)	(kN)	(kN)	(kN)			
SS-20-80	1901	1750	1732	1744	0.92	0.91	0.92
SS-50-80	1998	1753	1732	1875	0.88	0.87	0.94
SS-70-80	1959	1735	1702	1874	0.89	0.87	0.96

3 Numerical Study

Numerical study is performed using ABAQUS-v6.14. The initial out-of-straightness imperfection of the outer steel tube is incorporated as a half-sine wave profile through a prior buckling analysis. A scale factor of $L/4000$ is considered to mimic the measured magnitude of imperfection. Imperfection is assigned only for the outer steel tube and over-closure pressure is invoked at the steel-concrete interface. The steel tubes and concrete are modelled using shell (S4R) and solid (C3D8R) elements, respectively for the measured geometric properties. Elements are meshed in sizes less than $1/13^{th}$ of the steel tube width (Tao et al. 2013), and care is taken to avoid element distorsion. Loading and boundary conditions are invoked at end plates that are modelled using C3D8R element. Young's modulus and Poisson's ratio of $2x10^7$ N/mm^2 and 0.0001 respectively is assigned to the end plates to facilitate complete load transfer to the specimen with negligible end plate deformation. Tie constraint is used to simulate the weld connection between the end plates and the specimen. Surface-to-surface contact property is used

to define the compatibility between the steel tubes and concrete infill. A penalty friction coefficient of 0.25 is assigned in the tangential direction (Hu et al. 2003), and *hard contact* is assigned in the normal direction. Displacement-controlled loading and pinned boundary conditions (restraining x, y and z translations at base; and x and y translation at loading end) are assigned along the central line of end plates to simulate the test conditions. STATIC-GENERAL solver is used for analysis with *CONTACT CONTROL command to avoid convergence issues.

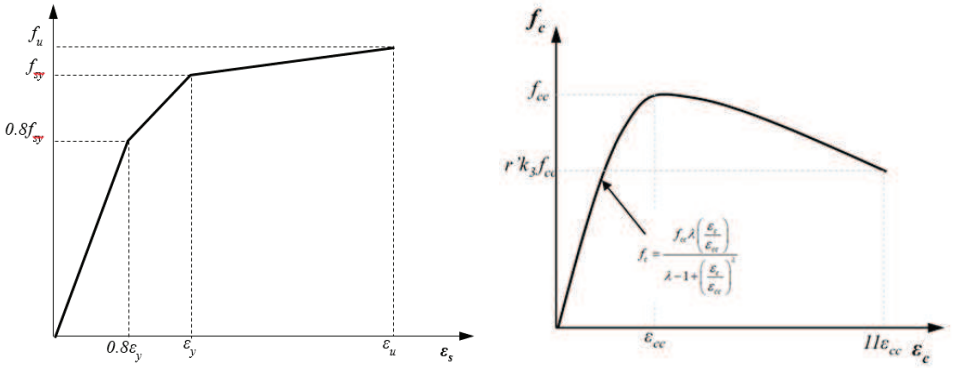

(a) (b)

Figure 3: Material model in numerical study. (a) Steel (b) Concrete

Tri-linear stress-strain model is assumed to define the material property of steel tubes (Fig. 3a), with pivotal points taken from the tension coupon test. Confined concrete model as shown in Fig. 3b is considered for the sandwiched concrete property. The pre-peak curve is based on Mander et al. (1988). The parameters of the model at pre-peak are defined based on the studies by Liang and Fragomeni (2009) for CFST. The post-peak curve is adopted from the numerical study by Pagoulatou et al. (2014). Drucker-Prager plasticity option available in ABAQUS library is used to define the plastic flow in the concrete model. A flow potential ratio of 0.8 and angle of friction of 20° are used for modelling, and the dilation angle is defined based on expressions recommended by Tao et al. (2013).

The axial compression behavior of the specimens from test and finite element output is compared in Figs. 4(a – c). The initial stiffness and the ultimate load from test and numerical predictions are in good agreement. The descending trend in the behavior curve also matches well with the test results. The finite element axial capacity prediction is close to the test axial capacity for all hollowness ratios of 0.7, 0.5 and 0.2 (around 6% error). Whereas, the code predictions give a conservative error of around 15%. Since the actual imperfection measured in the test specimens are used for developing the numerical model, the results are in good agreement. This shows that low initial imperfections increases the buckling capacity of long square CSDST columns. Nevertheless, the code prediction is less conservative for low hollowness specimen (SS-20-80). The finite element results of the failure pattern (global buckling) and the stress distribution across the cross-section at the peak-load is shown in Fig. 5(a – c).

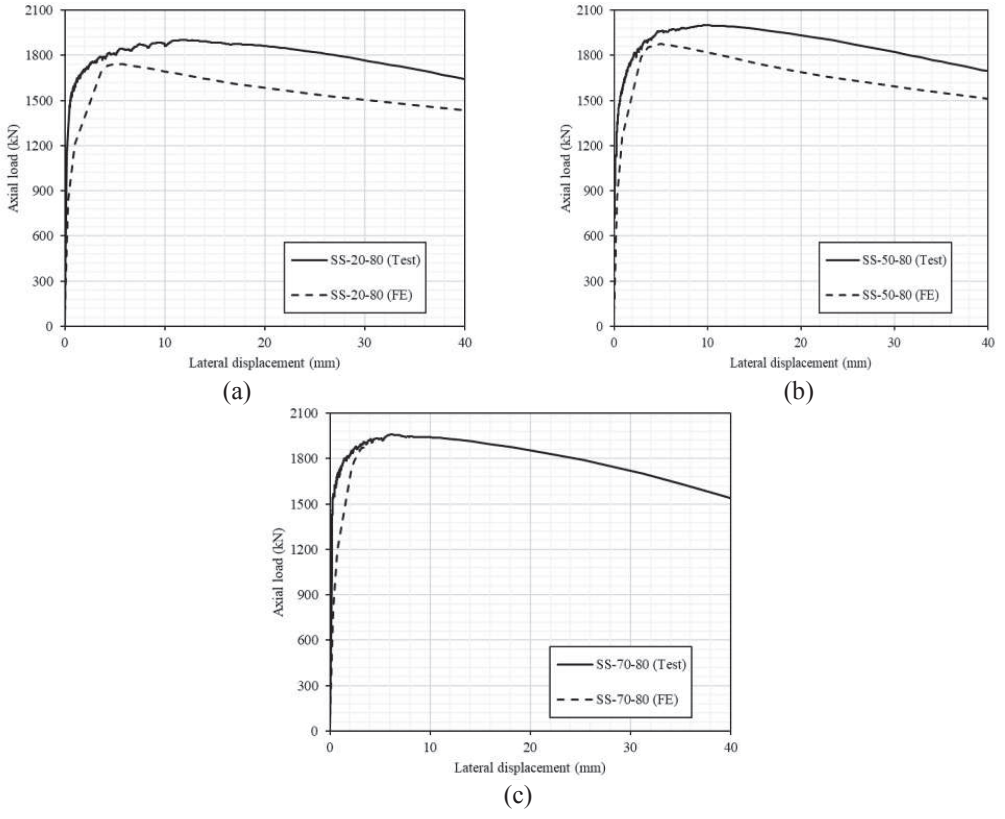

Figure 4: Comparison of test and finite element results for various hollowness ratios. (a) 0.2 (b) 0.5 (c) 0.7

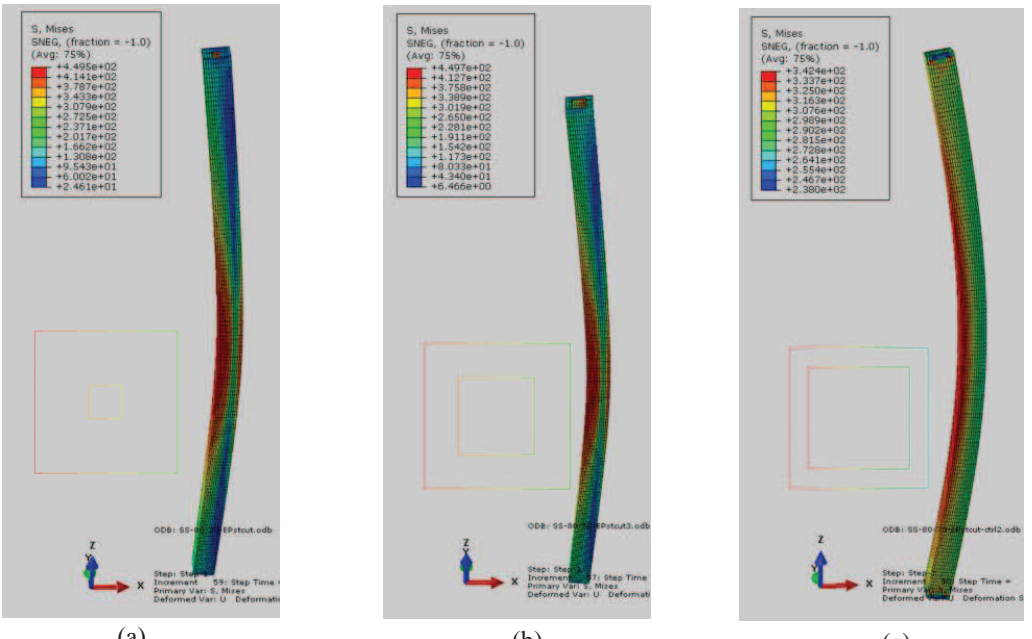

Figure 5: Finite element results of the failure pattern and stress distribution in the specimens. (a) SS-20-80 (b) SS-50-80 (c) SS-70-80

4 Conclusions

The salient conclusions from this study are enumerated as below.

- The global buckling behavior of square CSDST with high strength concrete infill is studied experimentally and numerically
- The test buckling capacity of the specimens are higher than code predictions due to low initial global imperfections in the outer steel tubes, particularly for specimens with higher hollowness ratios
- The finite element results are in good agreement with the test results as they are developed using actual initial imperfections in the test specimen
- The conservativeness in the code axial capacity prediction is lesser for specimens with low hollowness ratio (i.e. instability of long square CSDST columns is inversely related to the hollowness ratio of the cross-section).

Acknowledgements

The authors would like to extend their gratitude to TATAstructura for supplying the steel tubes for this experimental work. They are also very thankful for the lab staff at Structural engineering lab, IIT Madras for their help during the experimental process.

References

ANSI/AISC. (2016). "Specification for Structural Steel Buildings."

ASTM-E8/E8M. (2009). *Standard Test Methods for Tension Testing of Metallic Materials*. *ASTM*.

Eggemann, H. (2003). "Simplified Design of Composite Columns , Based on a Comparative Study of the Development of Building Regulations in Germany and the United States." 20.

Elchalakani, M., Zhao, X.-L., and Grzebieta, R. (2002). "Tests on concrete filled double-skin (CHS outer and SHS inner) composite short columns under axial compression." *Thin-Walled Structures*, 40(5), 415–441.

EN 1994-1-1. (2004). *Eurocode 4 : Design of composite steel and concrete structures Part 1-1 : General rules and rules for buildings*. *European Committee for Standardization*.

Essopjee, Y., and Dundu, M. (2015). "Performance of concrete-filled double-skin circular tubes in compression." *Composite Structures*, 133, 1276–1283.

Gardner, J. G., and Jacobson, E. R. (1967). "Structural Behavior of Concrete Filled Steel Tubes." *ACI Journal of Structural Division*, (64–38), 404–413.

Han, L.-H., Tao, Z., Huang, H., and Zhao, X.-L. (2004). "Concrete-filled double skin (SHS outer and CHS inner) steel tubular beam-columns." *Thin-Walled Structures*, 42(9), 1329–1355.

Hu, H., Huang, C., Wu, M.-H., and Wu, Y. (2003). "Nonlinear Analysis of Axially Loaded Concrete-Filled Tube Columns with Confinement Effect." *Journal of Structural Engineering (ASCE)*, 129(10), 1322–1329.

Huang, H., Han, L.-H., Tao, Z., and Zhao, X.-L. (2010). "Analytical behaviour of concrete-filled double skin steel tubular (CFDST) stub columns." *Journal of Constructional Steel Research*, 66(4), 542–555.

Knowles, R. B., and Park, R. (1969). "Strength of concrete filled steel tubular columns." *Jornal of Structural Division, ASCE*, 95(ST12), 2565–2587.

Liang, Q. Q., and Fragomeni, S. (2009). "Nonlinear analysis of circular concrete-filled steel tubular short columns under axial loading." *Journal of Constructional Steel Research*, 65(12), 2186–2196.

Lu, H., Zhao, X.-L., and Han, L.-H. (2011). "FE modelling and fire resistance design of concrete filled double skin tubular columns." *Journal of Constructional Steel Research*, 67(11), 1733–1748.

Mander, J. B., Priestley, M. J. N., and Park, R. (1988). "Theoretical stress-strain model for confined concrete." *Journal of Structural Engineering (ASCE)*, 114(8), 1804–1826.

Pagoulatou, M., Sheehan, T., Dai, X. H., and Lam, D. (2014). "Finite element analysis on the capacity of circular concrete-filled double-skin steel tubular (CFDST) stub columns." *Engineering Structures*, 72, 102–112.

Romero, M. L., Espinos, A., Portolés, J. M., Hospitaler, A., and Ibañez, C. (2015a). "Slender double-tube ultra-high strength concrete-filled tubular columns under ambient temperature and fire." *Engineering Structures*, 99, 536–545.

Romero, M. L., Portolés, J. M., Espinós, A., Pons, D., and Albero, V. (2015b). "Influence of Ultra-High Strength Concrete on Circular Concrete-Filled Dual Steel Columns." *11th International Conference on Advances in Steel and Concrete Composite Structures Tsinghua University, Beijing, China, December 3-5,*.

Sakino, K., Nakahara, H., Morino, S., and Nishiyama, I. (2004). "Behavior of Centrally Loaded Concrete-Filled Steel-Tube Short Columns." *Journal of Structural Engineering, ASCE*, 130(2), 180–188.

Tao, Z., Han, L.-H., and Zhao, X.-L. (2004). "Behaviour of concrete-filled double skin (CHS inner and CHS outer) steel tubular stub columns and beam-columns." *Journal of Constructional Steel Research*, 60(8), 1129–1158.

Tao, Z., Wang, Z., and Yu, Q. (2013). "Finite element modelling of concrete- filled steel stub columns under axial compression." *Journal of Constructional Steel Research*, 89, 121–131.

Uenaka, K., Kitoh, H., and Sonoda, K. (2010). "Concrete filled double skin circular stub columns under compression." *Thin-Walled Structures*, 48(1), 19–24.